








# Geophysical Research Letters<sup>®</sup>



## RESEARCH LETTER

10.1029/2022GL099964

## Rifting-Driven Magmatism Along the Dead Sea Continental Transform Fault

A. Haddad<sup>1</sup> , C. Chiarabba<sup>2</sup> , M. Lazar<sup>3</sup> , A. Mazzini<sup>4</sup> , A. Polonia<sup>5</sup> , L. Gasperini<sup>5</sup> , and M. Lupi<sup>1</sup> 

<sup>1</sup>Department of Earth Sciences, University of Geneva, Geneva, Switzerland, <sup>2</sup>Istituto Nazionale di Geofisica e Vulcanologia, INGV, Rome, Italy, <sup>3</sup>Department of Marine Geosciences, University of Haifa, Haifa, Israel, <sup>4</sup>Centre for Earth Evolution and Dynamics (CEED), University of Oslo, Oslo, Norway, <sup>5</sup>Institute of Marine Sciences, Italian National Research Council, Bologna, Italy

### Key Points:

- Magma emplaced along the Dead Sea Fault (DSF)
- Localized rifting along the segment of the DSF
- Occurrence of cooling magmas may reconcile several geophysical, geological and geochemical observations in around the Sea of Galilee

### Supporting Information:

Supporting Information may be found in the online version of this article.

### Correspondence to:

M. Lupi,  
[matteo.lupi@unige.ch](mailto:matteo.lupi@unige.ch)

### Citation:

Haddad, A., Chiarabba, C., Lazar, M., Mazzini, A., Polonia, A., Gasperini, L., & Lupi, M. (2023). Rifting-driven magmatism along the Dead Sea continental transform fault. *Geophysical Research Letters*, 50, e2022GL099964. <https://doi.org/10.1029/2022GL099964>

Received 15 JUN 2022  
Accepted 27 JAN 2023

**Abstract** The Dead Sea Fault (DSF) is a crustal-scale continental transform fault separating the African and the Arabian plates. Neogene to Quaternary volcanic activity is well-spread in Northern Israel. Yet, the origin of the magmas that fed the eruptions is still unpinned. Our local earthquake tomography depicts velocity distributions typical of rifting settings. At 9 km depth, a prominent high Vp/Vs anomaly marks the presence of cooling melts. We propose that protracted transtension along the DSF caused crustal thinning promoting the emplacement of magmatic bodies. Crustal emplacements of magmas in Northern Israel reconcile multiple observations, including the high geothermal gradient, the prominent magnetic anomalies and the traces of mantle-derived fluids in the springs across the Sea of Galilee. We provide a compelling evidence for rifting in segments of the DSF and identify the potential source of magmatism that fed part of the volcanic activity of the area.

**Plain Language Summary** The Dead Sea Fault (DSF) is a deep-reaching fault separating the African and the Arabian plates. Geologically recent volcanic activity is well-spread in Northern Israel but the origin of the magmas that fed the eruptions is yet to be found. We propose that protracted extensional motion along the DSF caused crustal thinning facilitating the emplacement of magmatic bodies in the crust. Our local earthquake tomography depicts velocity distributions typical of spreading margins. At 9 km depth, a prominent anomaly marks the presence of cooling melts. Crustal emplacements of magmas in Northern Israel reconcile multiple observations that are normally not common in sedimentary environments. The occurrence of magmas at depth would release fluids that would be compatible with the seismicity that sporadically affects the region. We provide a compelling evidence for rifting in segments of the DSF and identify the potential source of magmatism that fed part of the volcanic activity of the area. Our findings hold major implications for revisiting the natural hazard assessment of the Levant region.

## 1. Introduction

The Dead Sea Fault (DSF) is a crustal *sharp-cut* (Rosenthal et al., 2019) continental transform fault running for more than a thousand kilometers spreading to the Red Sea toward the South and bridging with collision in Turkey. This prominent geological feature was a major morphological corridor that allowed the migration of Hominids from Africa into Eurasia (Ben-avraham et al., 2005). The DSF, active since the Miocene (Matmon et al., 2003; Nuriel et al., 2012), is characterized by extensional structures such as the Dead Sea (Hofstetter et al., 2000) and the Sea of Galilee (SoG) (Hurwitz et al., 2000). The SoG developed within the Kinarot-Beit-Shean pull-apart basin where the sedimentary infill thickens toward the Eastern border of the DSF (Magri et al., 2015). Across Northern Israel and around the SoG, sediments alternate with magmatic formations as confirmed by deep-penetrating wells and geophysical data (including active seismic, magnetic field modeling and gravimetry) (Ben-Avraham et al., 2014; Eppelbaum et al., 2004; Reznikov et al., 2004; Sneh & Weinberger, 2003). Portions of the Levant volcanism (Figure 1b) flank the Eastern side of the SoG and the magmatic units extend across Syria, Jordan and Saudi Arabia (Weinstein & Heimann, 2017). Recently, magmatism and its source in the Kinneret-Kinarot basin have been reassessed using high-resolution mapping methods (Schattner et al., 2019, 2022; Segev et al., 2022). According these studies, there is no evidence for volcanic eruption centers within the basin. The authors conclude that magnetic anomalies probably represent subsurface basaltic bodies that flowed down-slope from the Golan Heights in the east and the Galilee in the west to fill the basin (Segev et al., 2022). The complex nature of

© 2023. The Authors.

This is an open access article under the terms of the [Creative Commons Attribution-NonCommercial-NoDerivs License](https://creativecommons.org/licenses/by-nc-nd/4.0/), which permits use and distribution in any medium, provided the original work is properly cited, the use is non-commercial and no modifications or adaptations are made.

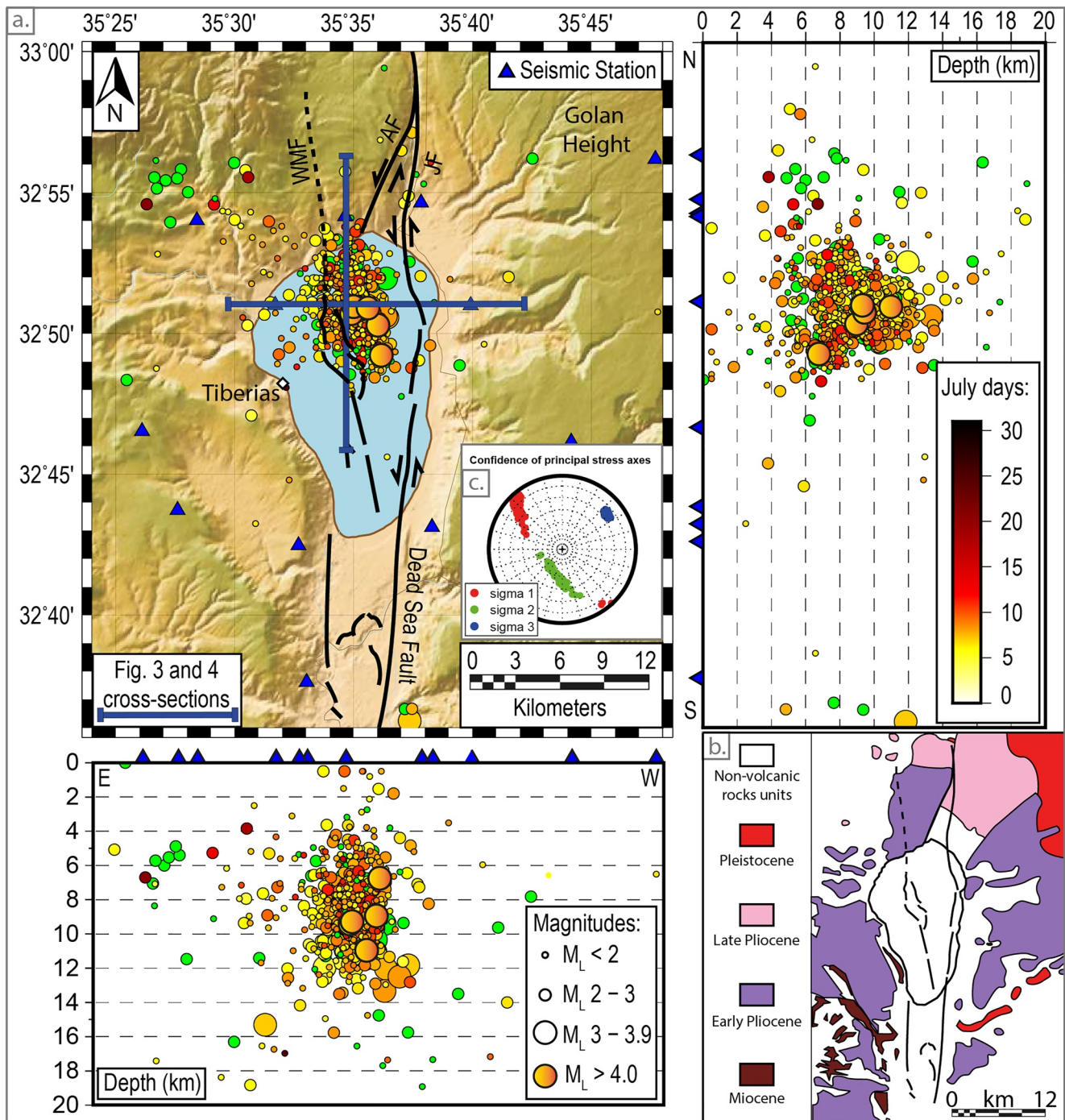


**Figure 1.** (a) Spatio-temporal distribution of earthquakes before and during the 2018 Sea of Galilee (SoG) seismic sequence. The color-scale shows the temporal evolution of the seismicity. Events in green occurred before the 2018 July sequence. The triangles indicate the seismic stations used for the tomography (Haddad et al., 2020). The tectonic setting was modified from previous authors (Garfunkel, 1981; Gasperini et al., 2019; Hurwitz et al., 2002; Matmon et al., 2010). WMF, Western Margin Fault; AF, Almogor Fault; DSTF, Dead Sea Transform Fault; JF, Jordan Fault. (b) Location of volcanic fields and their age in the SoG region (Schattner et al., 2019). (c) Distribution of the principal stress axes for all the events calculated with the *StressInverse* package (Vavryčuk, 2014). The sub-vertical  $\sigma_2$  suggest deformation with transensional mainly left-lateral (from Haddad et al. (2020)) kinematics.

magnetic anomalies in the SoG results from significant E-W trending deep-seated causative subsurface basalt bodies that were probably emplaced during the Pleistocene and a volcanic eruption center located in the Yarmouk River gorge in the south of the lake (Schattner et al., 2019). According to the authors, this provides the source of the basaltic flows and gabbro intrusions since 13 ma. The presence of magmas, despite not being proved yet

under the SoG, is also suggested by the mantle-derived isotopic signature of fluids sampled from the springs scattered around the SoG (Gasperini et al., 2019; Inguaggiato et al., 2016). The region is also characterized by an anomalously high heat flux ( $75\text{--}80\text{ mW m}^{-2}$ ) (Shalev et al., 2013). Around the SoG, the Moho is shallow, around 21 km depth (Koulakov & Sobolev, 2006; Mechie et al., 2013). Magnetic anomalies (Eppelbaum et al., 2004) and gravity data (Rosenthal et al., 2019; Segev et al., 2006) suggest the occurrence of denser basaltic units and a thicker sedimentary cover below the SoG, respectively. Tectonic deformation develops (c.f. creeping) on the scale of a few mm/yr (Hamiel et al., 2016) and it is more prominent on the eastern flank of the DSF in the SoG region.

## 2. Methods and Results

In July 2018 a seismic swarm struck the SoG (Haddad et al., 2020; Wetzler et al., 2019). The largest earthquake ( $M_L$  4.4) was followed for a month by more than 660 events that occurred at about 9 km depth (Haddad et al., 2020) (Figure 1). Parallel studies confirmed the swarm-like character of the seismic sequence (Wetzler et al., 2019) that is similar to what was already observed in 2013 (Wetzler et al., 2019). The proposed driving mechanisms suggest a causal relationship with either an exacerbated groundwater extraction from nearby wells (Wetzler et al., 2019) or tectonic activity driving faulting in the region (Haddad et al., 2020). Both studies agree on the important role of crustal fluids throughout the sequence and in suggesting that the regional deformation was masked by a local and more dominant stress field.

We used the catalog of a temporary seismic network deployed around the SoG (Haddad et al., 2020) that complemented six broadband stations of the Israel National Seismic Network to perform a local earthquake tomography (Figure 2). To calculate 3D Vp and Vp/Vs ratio velocity models we used the Simulps14 package (C. H. Thurber, 1983; C. Thurber & Eberhart-Phillips, 1999; Eberhart-Phillips, 1990; Haslinger et al., 1999). The 657 selected earthquakes have well-constrained focal depths (Haddad et al., 2020) and at least eight P-wave and three S-wave phase arrivals with highly-weighted values. Weight values for the phase picks were assigned using the PS-Picker algorithm (Baillard et al., 2014) (see also previous studies (Haddad et al., 2020)). A total of 607 earthquakes belong to the 2018 seismic sequence and 50 events were recorded before its occurrence (Figure 1). The calculation of the current stress regime by Haddad et al. (2020) shows sub-vertical  $\sigma_2$  suggesting lateral kinematics and a minor extensional component (Figure 2). This is in agreement with the tectonic context and stress regime imposed by the two left-stepping left-lateral strike-slip faults of the Kinerot-Beit-Shean pull-apart basin where the SoG develops (Figure 1).

Simulps14 inverts P- and S-waves phase arrival times solving simultaneously for earthquakes and Vp and Vp/Vs parameters (C. Thurber & Eberhart-Phillips, 1999). The initial velocity model that is used is obtained by the linear interpolation of starting values (from Haddad et al. (2020)) assigned to nodes of a 3D grid (Figure S1 in Supporting Information S1). The space between the nodes in the horizontal and vertical directions in the central area is 2 and 3 km, respectively (Figure 2). The spatial distribution of the processed earthquakes provides an excellent coverage of the northern part of the SoG (Figure 2). A spread function analysis was performed to identify the well-resolved regions (Figure 2) along with a synthetic test and a characteristic model test at 9 km depth (Figures S2 and S3 in Supporting Information S1).

The relocated seismicity occurs between 6 and 16 km depth and it is well-bounded on the Eastern side of the basin (Haddad et al., 2020) (Figure 1). The spatial distribution of P-wave velocities shows faster values in the northern part of the SoG. This region corresponds to the domain most affected by the 2018 seismic sequence (Figure 2). At 6 km depth, this high velocity region bounds the NE shore of the SoG and moves toward the center of the basin at greater depths where it becomes more prominent. At 15 km depth, the high Vp region is still visible in the center of the SoG. However, the resolution is not optimal at this depth and we avoid interpretations. We notice a striking correspondence between the distribution of high P-wave velocities shown in Figures 2 and 3a, the magnetic anomaly map of the SoG (Eppelbaum et al., 2004) and the negative Bouguer anomalies (Rosenthal et al., 2019) mapped in the region. The Vp/Vs ratio highlights low values in the upper crust (Figure 2e) that are interrupted at about 9 km depth by a prominent NW-striking region of high Vp/Vs ratio. The 2018 seismicity occurred precisely in this region (Figure 2f). At greater depths, such a sharp NW-striking discontinuity is still present but less prominent (Figure 2g).



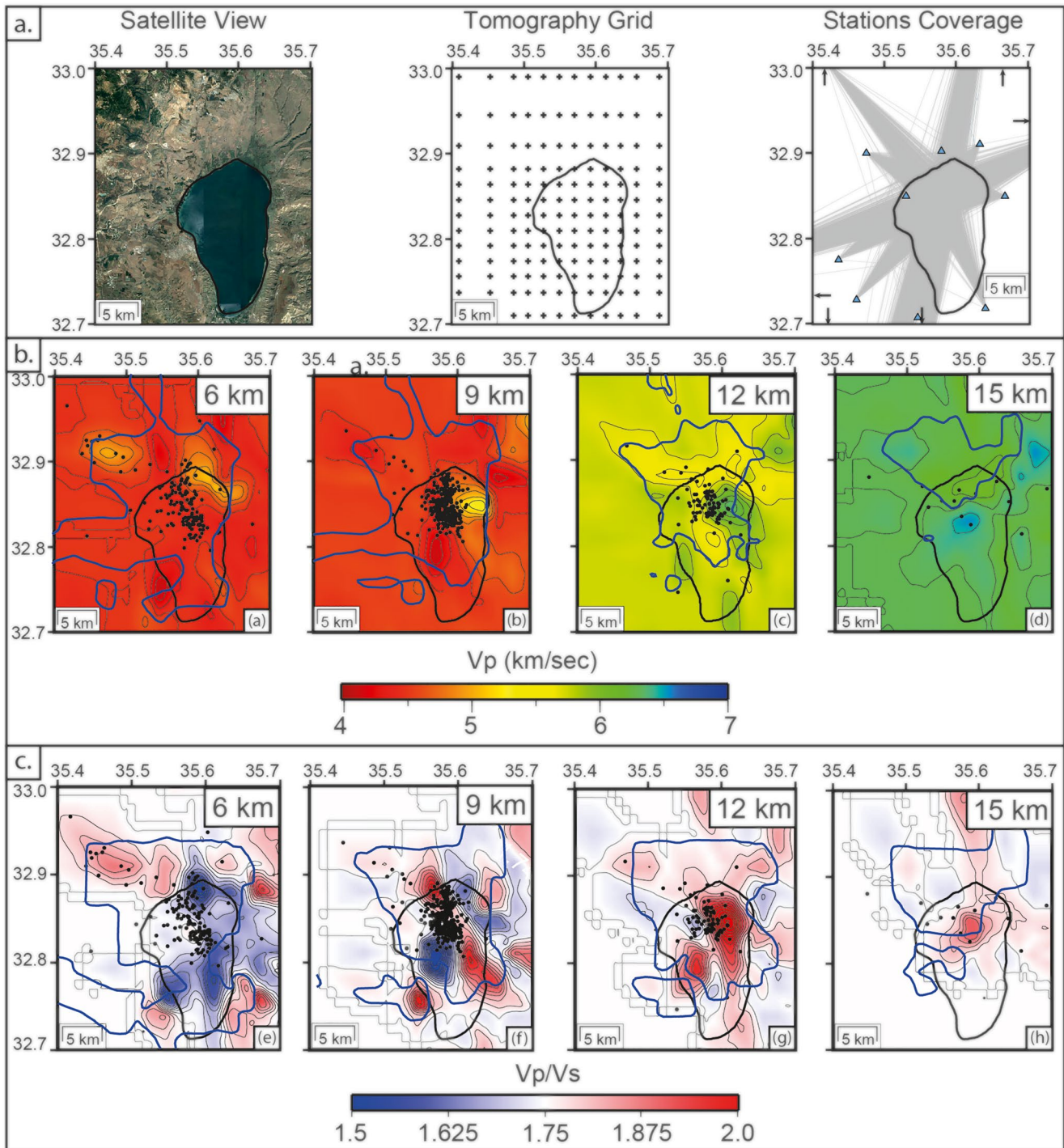


**Figure 2.** (a) Satellite Image, grid spacing and ray coverage. Grid spacing is 2 and 3 km in the horizontal and vertical direction, respectively. (b) Maps of P-wave velocities at 6, 9, 12, and 15 km depths. (c) Maps of  $V_p/V_s$  ratio at the same depths. The blue line limits the well-resolved volume (Spread Function = 3). Black dots correspond to the relocated earthquakes. Resolution tests are shown in Figure S2 in Supporting Information S1.

### 3. Discussion and Conclusions

The most striking feature of our velocity model is the high  $V_p/V_s$  ratio centered at around 9 km depth. High  $V_p/V_s$  regions with values of about two along continental transform faults may be ascribed to different lithologies and processes such as the presence of high- $V_p$  salt rocks (Yan et al., 2016), serpentinites and/or magmatic

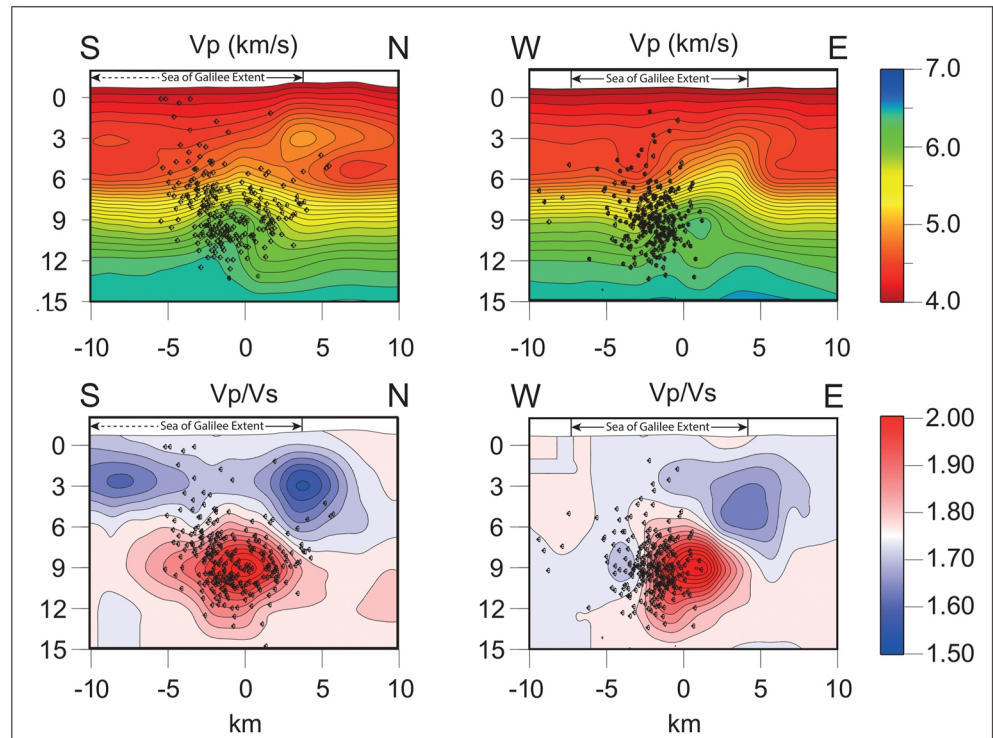


**Figure 3.** (a) Cross-sections of P-wave velocities and (b) Vp/Vs ratio. Positions of the cross-sections are shown in Figure 1. Black dots correspond to the relocated earthquakes.

intrusions (Grevemeyer et al., 2018). The occurrence of salt diapirs was already identified in the upper crust of Northern Israel (Dazel & Brouard, 2010; Inbar, 2012; Magri et al., 2015; Reznikov et al., 2004). However, the Zemah salt complex in the southern SoG and the Triassic units are suggested to be shallower than 6 km depth in this region, that is, well-inside the sedimentary cover. The occurrence of salt would not help explaining the occurrence of low Vs velocities. Moreover, salt would not cause positive magnetic anomalies as reported in the study region (Eppelbaum et al., 2004). An alternative hypothesis explaining high Vp/Vs ratios would relate to active serpentinization of mafic and ultramafic crustal rocks. In this scenario, low Vs would be related to the percolation of groundwaters along the DSF. However, the positive geothermal anomaly of the region implies upward convection instead of downwelling of fluid. Serpentinites would be inherited from the lithospheric mantle and buoyancy-triggered uprising of such lower density rocks along the DSF. Their development might be favored by the transtensional stress regime (Figure 1) that is also observed along the incipient rift zone of the Ionian Sea (Polonia et al., 2017). Inherited serpentinite along the displacement zone of a continental transform was also proposed along the San Andreas Fault (Ryberg et al., 2012). However, no evidence of serpentinites has been described for the DSF in the SoG and surrounding regions, therefore, we consider this hypothesis unlikely without further supporting data. The region with high Vp/Vs ratio runs parallel to the direction of the DSF hinting the central role that the crustal deformation may play.

To explain the observed velocity structure, we propose a comprehensive model consistent with other regional observations. We suggest that magmatism causes the high Vp/Vs ratio found at depth. Magma upwelling is driven by prolonged transtensional stress regime (Gasparini et al., 2019; Haddad et al., 2020; Hurwitz et al., 2002) (crustal-thinning) leading to localized rifting. Moderate passive rifting may facilitate asthenospheric rise (Segev et al., 2006) via lithostatic unloading, causing repeated, yet moderate and confined intrusions of melts in the upper crust. This is compatible with the shallow Moho found in the region at about 21 km depth (Mechie et al., 2013). In this context, magma and deep fluids rise through the crust flowing across the DSF. This scenario also explains the region's high heat flux as well as the mantle-derived signature of the fluids sampled around the SoG (Gasparini et al., 2019; Inguaggiato et al., 2016). The accumulation of magma in the middle to upper crust reconciles the swarm-like character of the 2018 and 2013 earthquake sequences and also addresses the masking of the dominant stress field suggested for the recent seismic events (Wetzler et al., 2019). Geology also provides support

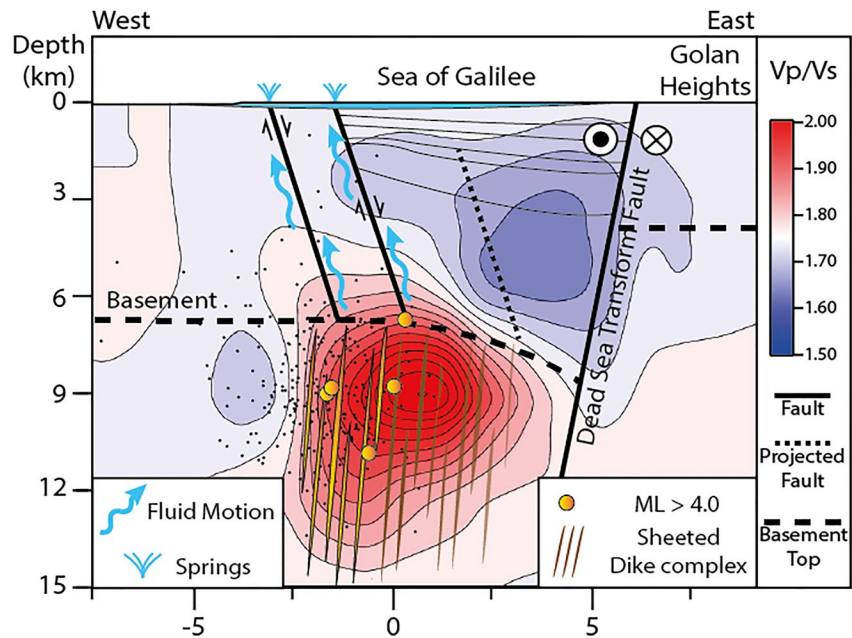


**Figure 4.** Conceptual model of the crustal structure beneath the Sea of Galilee. The black dots show the projected locations of the seismic events occurred in 2018. We propose that repeated and discrete intrusions of magma occur within the area characterized by  $V_p/V_s$  around two. Intrusions promoted by a slow and localized rifting-like protracted transtensional tectonics crystallize and release fluids causing the high  $V_p/V_s$  ratio. The arrows show the transtensional regime accommodated by a simplified fault system. The cross sections locations are shown on Figure 1. Faults locations and dips were extracted from geophysical data interpretation and maps (Garfunkel, 1981; Gasperini et al., 2019; Hurwitz et al., 2002; Matmon et al., 2010).

for the occurrence, at least in the past, of magmas at depth. Reconstructing the magmatic history of the region is not trivial. The Harrat Ash-Shaam volcanic field extends for a few hundreds kilometers eastwards (Weinstein & Heimann, 2017). While it seems to depart from the SoG segment of the DSF (Figure 1), magmatism of the Harrat ash-Shaam may not be strictly related to plate boundary processes. Bagley and Nyblade (2013) suggest that the African super plume may have driven magmatism in the region. Geophysical surveys across Northern Israel concur with the presence of Quaternary magmatic units beneath the SoG (Eppelbaum et al., 2004; Rosenthal et al., 2019). Furthermore, wells penetrate basaltic and pyroclastic units beneath the SoG at shallow depths (Rosenthal et al., 2019), that is, less than 1 km deep. Such a prominent magmatic activity may be driven by crustal thinning or at least by extensional kinematics. While transtension suggests the occurrence of a leaky transform (Garfunkel, 1981), Sadeh et al. (2012) shows minor regional stretching perpendicular to the plate boundary. Extensional processes may therefore be of local origin and due to specific geological processes occurring at depth. Indeed crustal thinning may be rapid and facilitate the rise in the crust of deep magmas (e.g., Christie-Blick and Biddle, 1985 and Smit et al., 2008).

While it is not possible to exclude an interplay between localized and regional transtensional deformation, the anomalously high heat flow around the SoG (Shalev et al., 2013) is consistent with the He signatures of groundwaters that suggest an efficient mix between percolating meteoric waters and upwelling mantle-derived fluids (Gasperini et al., 2019; Inguaggiato et al., 2016). This multidisciplinary set of information is in agreement with studies proposing the SoG as a rifting environment (Hurwitz et al., 2000; Smit et al., 2010). Recent seismological studies investigating the moderate magnitude earthquakes affecting the SoG segment of the DSF suggest swarm sequences (Haddad et al., 2020; Wetzler et al., 2019) where fluids interplay with tectonic deformation. In particular, it was proposed that local stress fields driving seismic sequences may overrule the large-scale tectonic stress field (Haddad et al., 2020; Wetzler et al., 2019). The velocity structure of the crust below the SoG recalls those of other rifting environments (Daly et al., 2008; Haslinger et al., 2001; Tryggvason et al., 2002). We therefore propose that the high P-wave velocities are caused by the presence of cooling magmas releasing fluids (low  $V_s$  velocities) (Figure 4). We notice that the distribution of the seismicity and the location of the high  $V_p/V_s$  anomaly well fit the studies of Sadeh et al. (2012) and Gomez et al. (2020) suggesting a similar depth for locked



region of this portion of the DSF. In turn, this drastically rules out the salt model proposed by Cohen et al. (2022). Indeed, the locking depths derived by geodetic models are often explained by the brittle-ductile transition (possibly due to the emplacement of magmas) and have been proposed for other similar geodynamic settings such as the San Andreas Fault (Smith-Konter et al., 2011).

Overall, our local earthquake tomography may help in understanding the evolution of other transform settings where the interplay between transtensional deformation and magmatism may promote the rise of deep fluids. While the association between strike-slip faulting and magmatism is well-established (Mathieu et al., 2011), less is known about localized rifting at continental transform margins. Yet, deep-reaching transform structures (e.g., the San Andreas and Anatolian Faults) are often associated with well-developed hydrothermal systems on the shoulders of the deforming zones (Berndt et al., 2016; Italiano et al., 2013; Mazzini et al., 2011). Our tomography substantiates a set of regional observations corroborating the evidence of repeated magmatic intrusions along a segment of the DSF (SoG) and suggests that this process may still be ongoing. Our study has relevant implications for a better understanding of the Levant volcanism and of the source of earthquakes occurring the SoG.

### Data Availability Statement

Permanent data of the Israel National Seismic Network (INSN) network belong to the Geological Survey of Israel and are freely accessible online through seeds. All the information about the INSN stations can be found at <https://www.fdsn.org/networks/detail/IS/>. Data recorded by the temporary stations can be found at <https://doi.org/10.5281/zenodo.3524185>.

### Acknowledgments

This work was jointly funded by multiple institutions including the COST Action FLOWS (ES1301) that is part of the Horizon 2020 program. Data will therefore be available once published. Antoine Haddad thanks the Department of Earth Sciences of the University of Geneva for salary support. Adriano Mazzini was funded by the European Research Council under the European Union's Seventh Framework Program grant agreement 308126 (LusiLab project, PI A. Mazzini). The authors also acknowledge the support from the Research Council of Norway through its Centers of Excellence funding scheme (project 223272) and the HOTMUD project (number 288299). Marion Alcanie, Guy Lang and Naama Sarid are thanked for their support in the field. Instruments have been acquired in the framework of the SNF project GENERATE (PI Matteo Lupi—Project 166900). The authors acknowledge the great contribution of three reviewers who very much helped streamlining and focusing this study.

### References

- Bagley, B., & Nyblade, A. A. (2013). Seismic anisotropy in eastern Africa, mantle flow, and the African Superplume. *Geophysical Research Letters*, *40*(8), 1500–1505. <https://doi.org/10.1002/grl.50315>
- Baillard, C., Crawford, W. C., Ballu, V., Hibert, C., & Mangeny, A. (2014). An automatic kurtosis-based P- and S-phase picker designed for local seismic networks. *Bulletin of the Seismological Society of America*, *104*(1), 394–409. <https://doi.org/10.1785/0120120347>
- Ben-avraham, Z., Lazar, M., Schattner, U., & Marco, S. (2005). The Dead Sea Fault and its effect on civilization. In *Sites the Journal of 20th Century Contemporary French Studies* (pp. 145–146).
- Ben-Avraham, Z., Rosenthal, M., Tibor, G., Navon, H., Wust-Bloch, H., Hofstetter, R., & Rybakov, M. (2014). Structure and tectonic development of the Kinneret Basin. In *Lake Kinneret* (pp. 19–38). Springer Netherlands. [https://doi.org/10.1007/978-94-017-8944-8\\_2](https://doi.org/10.1007/978-94-017-8944-8_2)
- Berndt, C., Hensen, C., Mortera-Gutierrez, C., Sarkar, S., Geilert, S., Schmidt, M., et al. (2016). Rifting under steam—How rift magmatism triggers methane venting from sedimentary basins. *Geology*, *44*(9), 767–770. <https://doi.org/10.1130/G38049.1>
- Christie-Blick, N., & Biddle, K. T. (1985). Deformation and basin formation along strike-slip faults.
- Cohen, O. B., Cesca, S., Dahm, T., Hofstetter, A., Hamiel, Y., & Agnon, A. (2022). Seismicity induced at the northern Dead Sea transform fault, Kinneret (sea of galilee) basin, by shallow creep involving a salt body. *Tectonics*, *41*, e2022TC0072047. <https://doi.org/10.1029/2022TC007247>
- Daly, E., Keir, D., Ebinger, C. J., Stuart, G. W., Bastow, I. D., & Ayele, A. (2008). Crustal tomographic imaging of a transitional continental rift: The Ethiopian rift. *Geophysical Journal International*, *172*(3), 1033–1048. <https://doi.org/10.1111/j.1365-246X.2007.03682.x>
- Dazel, O., & Brouard, B. (2010). Acoustics of porous materials. Lecture Notes, 6613(February).
- Eberhart-Phillips, D. (1990). Three-dimensional P and S velocity structure in the Coalinga region, California. *Journal of Geophysical Research*, *95*(B10), 15343. <https://doi.org/10.1029/jb095ib10p15343>
- Eppelbaum, L., Ben-Avraham, Z., Katz, Y., & Marco, S. (2004). Sea of Galilee: Comprehensive analysis of magnetic anomalies. *Israel Journal of Earth Sciences*, *53*(3–4), 151–171. <https://doi.org/10.1560/NQUR-CR5M-AQXX-KX1A>
- Garfunkel, Z. (1981). Internal structure of the Dead Sea leaky transform (rift) in relation to plate kinematics. *Tectonophysics*, *80*(1–4), 81–108. [https://doi.org/10.1016/0040-1951\(81\)90143-8](https://doi.org/10.1016/0040-1951(81)90143-8)
- Gasperini, L., Lazar, M., Mazzini, A., Polonia, A., Haddad, A., & Lupi, M. (2019). Neotectonics of the Sea of Galilee (North Israel): Implication for geodynamics and seismicity along the Dead Sea Fault system. *Science Report*, *10*, 11932. <https://doi.org/10.1038/s41598-020-67930-6>
- Gomez, F., Cochran, W. J., Yassminh, R., Jaafar, R., Reilinger, R., Floyd, M., et al. (2020). Fragmentation of the Sinai Plate indicated by spatial variation in present-day slip rate along the Dead Sea Fault system. *Geophysical Journal International*, *221*(3), 1913–1940. <https://doi.org/10.1093/gji/ggaa095>
- Grevemeyer, I., Hayman, N. W., Peirce, C., Schwardt, M., Van Avendonk, H. J., Dannowski, A., & Papenberg, C. (2018). Episodic magmatism and serpentinized mantle exhumation at an ultraslow-spreading centre. *Nature Geoscience*, *11*(6), 444–448. <https://doi.org/10.1038/s41561-018-0124-6>
- Haddad, A., Alcanie, M., Zahradnik, J., Lazar, M., Antunes, V., Gasperini, L., et al. (2020). Tectonics of the Dead Sea fault driving the July 2018 seismic swarm in the sea of galilee (Lake Kinneret), Israel. *Journal of Geophysical Research: Solid Earth*, *125*(10), e2019JB018963. <https://doi.org/10.1029/2019JB018963>
- Hamiel, Y., Piatibratova, O., & Mizrahi, Y. (2016). Creep along the northern Jordan Valley section of the Dead Sea Fault. *Geophysical Research Letters*, *43*(6), 2494–2501. <https://doi.org/10.1002/2016GL067913>
- Haslinger, F., Kissling, E., Ansorge, J., Hatzfeld, D., Papadimitriou, E., Karakostas, V., et al. (1999). 3D crustal structure from local earthquake tomography around the Gulf of Arta (Ionian region, NW Greece). *Tectonophysics*, *304*(3), 201–218. [https://doi.org/10.1016/S0040-1951\(98\)00298-4](https://doi.org/10.1016/S0040-1951(98)00298-4)
- Haslinger, F., Thurber, C., Mandernach, M., & Okubo, P. (2001). Tomographic image of P-velocity structure beneath Kilauea's East Rift Zone and South Flank: Seismic evidence for a deep magma body. *Geophysical Research Letters*, *28*(2), 375–378. <https://doi.org/10.1029/2000GL012018>

- Hofstetter, A., Dorbath, C., Rybakov, M., & Goldshmidt, V. (2000). Crustal and upper mantle structure across the Dead Sea rift and Israel from teleseismic P-wave tomography and gravity data. *Tectonophysics*, 327(1–2), 37–59. [https://doi.org/10.1016/S0040-1951\(00\)00161-X](https://doi.org/10.1016/S0040-1951(00)00161-X)
- Hurwitz, S., Garfunkel, Z., Ben-Gai, Y., Reznikov, M., Rotstein, Y., & Gvirtzman, H. (2002). The tectonic framework of a complex pull-apart basin: Seismic reflection observations in the Sea of Galilee, Dead Sea transform. *Tectonophysics*, 359(3–4), 289–306. [https://doi.org/10.1016/S0040-1951\(02\)00516-4](https://doi.org/10.1016/S0040-1951(02)00516-4)
- Hurwitz, S., Stanislavsky, E., Lyakhovsky, V., & Gvirtzman, H. (2000). Transient groundwater-lake interactions in a continental rift: Sea of Galilee, Israel. *GSA Bulletin*, 112(11), 1694–1702. [https://doi.org/10.1130/0016-7606\(2000\)112\(1694:glia\)2.0.co;2](https://doi.org/10.1130/0016-7606(2000)112(1694:glia)2.0.co;2)
- Inbar, N. (2012). *The evaporitic subsurface body of Kinnarot Basin* (Unpublished doctoral dissertation). Tel Aviv University.
- Inguaggiato, C., Censi, P., D'Alessandro, W., & Zuddas, P. (2016). Geochemical characterisation of gases along the Dead Sea Rift: Evidence of mantle-CO<sub>2</sub> degassing. *Journal of Volcanology and Geothermal Research*, 320, 50–57. <https://doi.org/10.1016/j.jvolgeores.2016.04.008>
- Italiano, F., Sasmaz, A., Yuce, G., & Okan, O. O. (2013). Thermal fluids along the East Anatolian Fault Zone (EAFZ): Geochemical features and relationships with the tectonic setting. *Chemical Geology*, 339, 103–114. <https://doi.org/10.1016/J.CHEMGEO.2012.07.027>
- Koulakov, I., & Sobolev, S. V. (2006). Moho depth and three-dimensional P and S structure of the crust and uppermost mantle in the Eastern Mediterranean and Middle East derived from tomographic inversion of local ISC data. *Geophysical Journal International*, 164(1), 218–235. <https://doi.org/10.1111/j.1365-246X.2005.02791.x>
- Magri, F., Inbar, N., Siebert, C., Rosenthal, E., Guttman, J., & Möller, P. (2015). Transient simulations of large-scale hydrogeological processes causing temperature and salinity anomalies in the Tiberias Basin. *Journal of Hydrology*, 520, 342–355. <https://doi.org/10.1016/j.jhydrol.2014.11.055>
- Mathieu, L., van Wyk de Vries, B., Pilato, M., & Troll, V. R. (2011). The interaction between volcanoes and strike-slip, transtensional and transpressional fault zones: Analogue models and natural examples. *Journal of Structural Geology*, 33(5), 898–906. <https://doi.org/10.1016/j.jsg.2011.03.003>
- Matmon, A., Katz, O., Shaar, R., Ron, H., Porat, N., & Agnon, A. (2010). Timing of relay ramp growth and normal fault linkage, Upper Galilee, northern Israel. *Tectonics*, 29(2), 1–13. <https://doi.org/10.1029/2009TC002510>
- Matmon, A., Wdowinski, S., & Hall, J. K. (2003). Morphological and structural relations in the Galilee extensional domain, northern Israel. *Tectonophysics*, 371(1–4), 223–241. [https://doi.org/10.1016/S0040-1951\(03\)00237-3](https://doi.org/10.1016/S0040-1951(03)00237-3)
- Mazzini, A., Svensen, H., Etiope, G., Onderdonk, N., & Banks, D. (2011). Fluid origin, gas fluxes and plumbing system in the sediment-hosted Salton Sea Geothermal System (California, USA). *Journal of Volcanology and Geothermal Research*, 205(3–4), 67–83. <https://doi.org/10.1016/j.jvolgeores.2011.05.008>
- Mechie, J., Ben-Avraham, Z., Weber, M., Götz, H.-J., Koulakov, I., Mohsen, A., & Stiller, M. (2013). The distribution of Moho depths beneath the Arabian Plate and margins. *Tectonophysics*, 609, 234–249. <https://doi.org/10.1016/j.tecto.2012.11.015>
- Nuriel, P., Weinberger, R., Rosenbaum, G., Golding, S. D., Zhao, J.-X., Uysal, I. T., et al. (2012). Timing and mechanism of late-pleistocene calcite vein formation across the Dead Sea Fault zone, northern Israel. *Journal of Structural Geology*, 36, 43–54. <https://doi.org/10.1016/j.jsg.2011.12.010>
- Polonia, A., Torelli, L., Gasperini, L., Cocchi, L., Muccini, F., Bonatti, E., et al. (2017). Lower plate Serpentinite Diapirism in the Calabrian Arc subduction complex. *Nature Communications*, 8(1), 2172. <https://doi.org/10.1038/s41467-017-02273-x>
- Reznikov, M., Ben-Avraham, Z., Garfunkel, Z., Gvirtzman, H., & Rotstein, Y. (2004). Structural and stratigraphic framework of Lake Kinneret. *Israel Journal of Earth Sciences*, 53(3–4), 131–149. <https://doi.org/10.1560/QY1W-VVRM-FLNK-C9M9>
- Rosenthal, M., Ben-Avraham, Z., & Schattner, U. (2019). Almost a sharp cut—A case study of the cross point between a continental transform and a rift, based on 3D gravity modeling. *Tectonophysics*, 761, 46–64. <https://doi.org/10.1016/j.tecto.2019.04.012>
- Ryberg, T., Hole, J. A., Fuis, G. S., Rymer, M. J., Bleibinhaus, F., Stromeyer, D., & Bauer, K. (2012). Tomographic V p and V s structure of the California Central Coast Ranges, in the vicinity of SAFOD, from controlled-source seismic data. *Geophysical Journal International*, 190(3), 1341–1360. <https://doi.org/10.1111/j.1365-246X.2012.05585.x>
- Sadeh, M., Hamiel, Y., Ziv, A., Bock, Y., Fang, P., & Wdowinski, S. (2012). Crustal deformation along the Dead Sea transform and the Carmel fault inferred from 12 years of GPS measurements. *Journal of Geophysical Research*, 117(B8), B08410. <https://doi.org/10.1029/2012jg009241>
- Schattner, U., Segev, A., Mikhailov, V., Rybakov, M., & Lyakhovsky, V. (2019). Magnetic signature of the Kinneret–Kinnarot tectonic basin along the Dead Sea Transform, northern Israel. *Pure and Applied Geophysics*, 176(10), 4383–4399. <https://doi.org/10.1007/S00024-019-02211-6>
- Schattner, U., Segev, A., Mikhailov, V., Rybakov, M., & Lyakhovsky, V. (2022). Detailed regional magnetic mapping on a bike, a case study from northern Israel. *Pure and Applied Geophysics*, 179(8), 2769–2795. <https://doi.org/10.1007/S00024-022-03100-1>
- Segev, A., Reznik, I. J., & Schattner, U. (2022). Miocene to sub-recent magmatism at the intersection between the Dead Sea Transform and the Ash Shaam volcanic field: Evidence from the Yarmouk River gorge and vicinity. *Geological Magazine*, 159(4), 469–493. <https://doi.org/10.1017/S0016756821001072>
- Segev, A., Rybakov, M., Lyakhovsky, V., Hofstetter, A., Tibor, G., Goldshmidt, V., & Ben Avraham, Z. (2006). The structure, isostasy and gravity field of the Levant continental margin and the southeast Mediterranean area. *Tectonophysics*, 425(1–4), 137–157. <https://doi.org/10.1016/j.tecto.2006.07.010>
- Shalev, E., Lyakhovsky, V., Weinstein, Y., & Ben-Avraham, Z. (2013). The thermal structure of Israel and the Dead Sea Fault. *Tectonophysics*, 602, 69–77. <https://doi.org/10.1016/j.tecto.2012.09.011>
- Smit, J., Brun, J.-P., Cloetingh, S., & Ben-Avraham, Z. (2008). Pull-apart basin formation and development in narrow transform zones with application to the Dead Sea Basin. *Tectonics*, 27(6), TC6018. <https://doi.org/10.1029/2007tc002119>
- Smit, J., Brun, J.-P., Cloetingh, S., & Ben-Avraham, Z. (2010). The rift-like structure and asymmetry of the Dead Sea Fault. *Earth and Planetary Science Letters*, 290(1–2), 74–82. <https://doi.org/10.1016/j.epsl.2009.11.060>
- Smith-Konter, B. R., Sandwell, D. T., & Shearer, P. (2011). Locking depths estimated from geodesy and seismology along the San Andreas fault system: Implications for seismic moment release. *Journal of Geophysical Research*, 116(B6), B06401. <https://doi.org/10.1029/2010jb008117>
- Sneh, A., & Weinberger, R. (2003). Geology of the Metulla quadrangle, northern Israel: Implications for the offset along the Dead Sea Rift. *Israel Journal of Earth Sciences*, 52(3–4), 123–138. <https://doi.org/10.1560/1G3J-NX0H-KBL3-RUY9>
- Thurber, C., & Eberhart-Phillips, D. (1999). Local earthquake tomography with flexible gridding. *Computers & Geosciences*, 25(7), 809–818. [https://doi.org/10.1016/S0098-3004\(99\)00007-2](https://doi.org/10.1016/S0098-3004(99)00007-2)
- Thurber, C. H. (1983). Earthquake locations and three-dimensional crustal structure in the Coyote Lake area, central California (USA). *Journal of Geophysical Research*, 88(B10), 8226. <https://doi.org/10.1029/JB088iB10p08226>
- Tryggvason, A., Rögnvaldsson, S. T., & Flóvenz, Ó. G. (2002). Three-dimensional imaging of the P- and S-wave velocity structure and earthquake locations beneath Southwest Iceland. *Geophysical Journal International*, 151(3), 848–866. <https://doi.org/10.1046/j.1365-246X.2002.01812.x>
- Vavryčuk, V. (2014). Iterative joint inversion for stress and fault orientations from focal mechanisms. *Geophysical Journal International*, 199(1), 69–77. <https://doi.org/10.1093/gji/ggu224>



- Weinstein, Y., & Heimann, A. (2017). Spatial and temporal patterns of late Cenozoic volcanism in the Levant. In *Quaternary of the Levant* (pp. 45–52). Cambridge University Press. <https://doi.org/10.1017/9781316106754.005>
- Wetzler, N., Shalev, E., Göbel, T., Amelung, F., Kurzon, I., Lyakhovsky, V., & Brodsky, E. E. (2019). Earthquake swarms triggered by groundwater extraction near the Dead Sea Fault. *Geophysical Research Letters*, *46*(14), 8056–8063. <https://doi.org/10.1029/2019GL083491>
- Yan, F., Hua Han, D., Yao, Q., & Chen, X. L. (2016). Seismic velocities of halite salt: Anisotropy, heterogeneity, dispersion, temperature, and pressure effects. *Geophysics*, *81*(4), D293–D301. <https://doi.org/10.1190/GEO2015-0476.1>

### References From the Supporting Information

- Thompson, G., & Reyes, C. (2018). GISMO - A seismic data analysis toolbox for MATLAB [software package]. GISMO. Retrieved from <https://geoscience-community-codes.github.io/GISMO/>